



## Studies of the Decay $B^\pm \rightarrow D_{CP}K^\pm$

K. Abe,<sup>9</sup> K. Abe,<sup>44</sup> N. Abe,<sup>47</sup> R. Abe,<sup>30</sup> T. Abe,<sup>45</sup> Byoung Sup Ahn,<sup>16</sup> H. Aihara,<sup>46</sup> M. Akatsu,<sup>23</sup> Y. Asano,<sup>51</sup> T. Aso,<sup>50</sup> V. Aulchenko,<sup>2</sup> T. Aushev,<sup>13</sup> A. M. Bakich,<sup>41</sup> Y. Ban,<sup>34</sup> P. K. Behera,<sup>52</sup> I. Bizjak,<sup>14</sup> A. Bondar,<sup>2</sup> A. Bozek,<sup>28</sup> M. Bračko,<sup>21,14</sup> T. E. Browder,<sup>8</sup> B. C. K. Casey,<sup>8</sup> M.-C. Chang,<sup>27</sup> P. Chang,<sup>27</sup> Y. Chao,<sup>27</sup> B. G. Cheon,<sup>40</sup> R. Chistov,<sup>13</sup> Y. Choi,<sup>40</sup> Y. K. Choi,<sup>40</sup> M. Danilov,<sup>13</sup> L. Y. Dong,<sup>11</sup> A. Drutskoy,<sup>13</sup> S. Eidelman,<sup>2</sup> V. Eiges,<sup>13</sup> Y. Enari,<sup>23</sup> F. Fang,<sup>8</sup> H. Fujii,<sup>9</sup> C. Fukunaga,<sup>48</sup> N. Gabyshev,<sup>9</sup> A. Garmash,<sup>2,9</sup> T. Gershon,<sup>9</sup> B. Golob,<sup>20,14</sup> A. Gordon,<sup>22</sup> R. Guo,<sup>25</sup> J. Haba,<sup>9</sup> T. Hara,<sup>32</sup> Y. Harada,<sup>30</sup> H. Hayashii,<sup>24</sup> M. Hazumi,<sup>9</sup> E. M. Heenan,<sup>22</sup> I. Higuchi,<sup>45</sup> T. Higuchi,<sup>46</sup> L. Hinz,<sup>19</sup> T. Hokuue,<sup>23</sup> Y. Hoshi,<sup>44</sup> S. R. Hou,<sup>27</sup> W.-S. Hou,<sup>27</sup> S.-C. Hsu,<sup>27</sup> H.-C. Huang,<sup>27</sup> T. Igaki,<sup>23</sup> Y. Igarashi,<sup>9</sup> T. Iijima,<sup>23</sup> K. Inami,<sup>23</sup> A. Ishikawa,<sup>23</sup> H. Ishino,<sup>47</sup> R. Itoh,<sup>9</sup> H. Iwasaki,<sup>9</sup> Y. Iwasaki,<sup>9</sup> H. K. Jang,<sup>39</sup> J. H. Kang,<sup>55</sup> J. S. Kang,<sup>16</sup> N. Katayama,<sup>9</sup> Y. Kawakami,<sup>23</sup> N. Kawamura,<sup>1</sup> T. Kawasaki,<sup>30</sup> H. Kichimi,<sup>9</sup> D. W. Kim,<sup>40</sup> Heejong Kim,<sup>55</sup> H. J. Kim,<sup>55</sup> H. O. Kim,<sup>40</sup> Hyunwoo Kim,<sup>16</sup> S. K. Kim,<sup>39</sup> T. H. Kim,<sup>55</sup> K. Kinoshita,<sup>5</sup> S. Korpar,<sup>21,14</sup> P. Krizan,<sup>20,14</sup> P. Krokovny,<sup>2</sup> R. Kulasiri,<sup>5</sup> S. Kumar,<sup>33</sup> A. Kuzmin,<sup>2</sup> Y.-J. Kwon,<sup>55</sup> J. S. Lange,<sup>6,36</sup> G. Leder,<sup>12</sup> S. H. Lee,<sup>39</sup> J. Li,<sup>38</sup> A. Limosani,<sup>22</sup> D. Liventsev,<sup>13</sup> R.-S. Lu,<sup>27</sup> J. MacNaughton,<sup>12</sup> G. Majumder,<sup>42</sup> F. Mandl,<sup>12</sup> D. Marlow,<sup>35</sup> T. Matsuishi,<sup>23</sup> S. Matsumoto,<sup>4</sup> T. Matsumoto,<sup>48</sup> W. Mitaroff,<sup>12</sup> K. Miyabayashi,<sup>24</sup> Y. Miyabayashi,<sup>23</sup> H. Miyake,<sup>32</sup> H. Miyata,<sup>30</sup> G. R. Moloney,<sup>22</sup> T. Mori,<sup>4</sup> A. Murakami,<sup>37</sup> T. Nagamine,<sup>45</sup> Y. Nagasaka,<sup>10</sup> T. Nakadaira,<sup>46</sup> E. Nakano,<sup>31</sup> M. Nakao,<sup>9</sup> J. W. Nam,<sup>40</sup> Z. Natkaniec,<sup>28</sup> K. Neichi,<sup>44</sup> S. Nishida,<sup>17</sup> O. Nitoh,<sup>49</sup> S. Noguchi,<sup>24</sup> T. Nozaki,<sup>9</sup> S. Ogawa,<sup>43</sup> T. Ohshima,<sup>23</sup> T. Okabe,<sup>23</sup> S. Okuno,<sup>15</sup> S. L. Olsen,<sup>8</sup> Y. Onuki,<sup>30</sup> W. Ostrowicz,<sup>28</sup> H. Ozaki,<sup>9</sup> P. Pakhlov,<sup>13</sup> H. Palka,<sup>28</sup> C. W. Park,<sup>16</sup> H. Park,<sup>18</sup> L. S. Peak,<sup>41</sup> J.-P. Perroud,<sup>19</sup> M. Peters,<sup>8</sup> L. E. Piilonen,<sup>53</sup> J. L. Rodriguez,<sup>8</sup> F. J. Ronga,<sup>19</sup> N. Root,<sup>2</sup> M. Rozanska,<sup>28</sup> K. Rybicki,<sup>28</sup> H. Sagawa,<sup>9</sup> S. Saitoh,<sup>9</sup> Y. Sakai,<sup>9</sup> M. Satpathy,<sup>52</sup> A. Satpathy,<sup>9,5</sup> O. Schneider,<sup>19</sup> S. Schrenk,<sup>5</sup> C. Schwanda,<sup>9,12</sup> S. Semenov,<sup>13</sup> K. Senyo,<sup>23</sup> R. Seuster,<sup>8</sup> M. E. Sevir,<sup>22</sup> H. Shibuya,<sup>43</sup> B. Shwartz,<sup>2</sup> V. Sidorov,<sup>2</sup> J. B. Singh,<sup>33</sup> S. Stanič,<sup>51,\*</sup> M. Starič,<sup>14</sup> A. Sugi,<sup>23</sup> A. Sugiyama,<sup>23</sup> K. Sumisawa,<sup>9</sup> T. Sumiyoshi,<sup>48</sup> K. Suzuki,<sup>9</sup> S. Suzuki,<sup>54</sup> S. Y. Suzuki,<sup>9</sup> T. Takahashi,<sup>31</sup> F. Takasaki,<sup>9</sup> K. Tamai,<sup>9</sup> N. Tamura,<sup>30</sup> J. Tanaka,<sup>46</sup> M. Tanaka,<sup>9</sup> G. N. Taylor,<sup>22</sup> Y. Teramoto,<sup>31</sup> S. Tokuda,<sup>23</sup> S. N. Tovey,<sup>22</sup> K. Trabelsi,<sup>8</sup> T. Tsuboyama,<sup>9</sup> T. Tsukamoto,<sup>9</sup> S. Uehara,<sup>9</sup> K. Ueno,<sup>27</sup> Y. Unno,<sup>3</sup> S. Uno,<sup>9</sup> Y. Ushiroda,<sup>9</sup> G. Varner,<sup>8</sup> K. E. Varvell,<sup>41</sup> C. C. Wang,<sup>27</sup> C. H. Wang,<sup>26</sup> J. G. Wang,<sup>53</sup> M.-Z. Wang,<sup>27</sup> Y. Watanabe,<sup>47</sup> E. Won,<sup>16</sup> B. D. Yabsley,<sup>53</sup> Y. Yamada,<sup>9</sup> A. Yamaguchi,<sup>45</sup> Y. Yamashita,<sup>29</sup> M. Yamauchi,<sup>9</sup> H. Yanai,<sup>30</sup> P. Yeh,<sup>27</sup> Y. Yuan,<sup>11</sup> Y. Yusa,<sup>45</sup> J. Zhang,<sup>51</sup> Z. P. Zhang,<sup>38</sup> Y. Zheng,<sup>8</sup> V. Zhilich,<sup>2</sup> and D. Žontar<sup>51</sup>

(The Belle Collaboration)

<sup>1</sup>*Aomori University, Aomori*

<sup>2</sup>*Budker Institute of Nuclear Physics, Novosibirsk*

- <sup>3</sup>*Chiba University, Chiba*
- <sup>4</sup>*Chuo University, Tokyo*
- <sup>5</sup>*University of Cincinnati, Cincinnati OH*
- <sup>6</sup>*University of Frankfurt, Frankfurt*
- <sup>7</sup>*Gyeongsang National University, Chinju*
- <sup>8</sup>*University of Hawaii, Honolulu HI*
- <sup>9</sup>*High Energy Accelerator Research Organization (KEK), Tsukuba*
- <sup>10</sup>*Hiroshima Institute of Technology, Hiroshima*
- <sup>11</sup>*Institute of High Energy Physics,  
Chinese Academy of Sciences, Beijing*
- <sup>12</sup>*Institute of High Energy Physics, Vienna*
- <sup>13</sup>*Institute for Theoretical and Experimental Physics, Moscow*
- <sup>14</sup>*J. Stefan Institute, Ljubljana*
- <sup>15</sup>*Kanagawa University, Yokohama*
- <sup>16</sup>*Korea University, Seoul*
- <sup>17</sup>*Kyoto University, Kyoto*
- <sup>18</sup>*Kyungpook National University, Taegu*
- <sup>19</sup>*Institut de Physique des Hautes Énergies, Université de Lausanne, Lausanne*
- <sup>20</sup>*University of Ljubljana, Ljubljana*
- <sup>21</sup>*University of Maribor, Maribor*
- <sup>22</sup>*University of Melbourne, Victoria*
- <sup>23</sup>*Nagoya University, Nagoya*
- <sup>24</sup>*Nara Women's University, Nara*
- <sup>25</sup>*National Kaohsiung Normal University, Kaohsiung*
- <sup>26</sup>*National Lien-Ho Institute of Technology, Miao Li*
- <sup>27</sup>*National Taiwan University, Taipei*
- <sup>28</sup>*H. Niewodniczanski Institute of Nuclear Physics, Krakow*
- <sup>29</sup>*Nihon Dental College, Niigata*
- <sup>30</sup>*Niigata University, Niigata*
- <sup>31</sup>*Osaka City University, Osaka*
- <sup>32</sup>*Osaka University, Osaka*
- <sup>33</sup>*Panjab University, Chandigarh*
- <sup>34</sup>*Peking University, Beijing*
- <sup>35</sup>*Princeton University, Princeton NJ*
- <sup>36</sup>*RIKEN BNL Research Center, Brookhaven NY*
- <sup>37</sup>*Saga University, Saga*
- <sup>38</sup>*University of Science and Technology of China, Hefei*
- <sup>39</sup>*Seoul National University, Seoul*
- <sup>40</sup>*Sungkyunkwan University, Suwon*
- <sup>41</sup>*University of Sydney, Sydney NSW*
- <sup>42</sup>*Tata Institute of Fundamental Research, Bombay*
- <sup>43</sup>*Toho University, Funabashi*
- <sup>44</sup>*Tohoku Gakuin University, Tagajo*
- <sup>45</sup>*Tohoku University, Sendai*
- <sup>46</sup>*University of Tokyo, Tokyo*
- <sup>47</sup>*Tokyo Institute of Technology, Tokyo*
- <sup>48</sup>*Tokyo Metropolitan University, Tokyo*

<sup>49</sup>*Tokyo University of Agriculture and Technology, Tokyo*  
<sup>50</sup>*Toyama National College of Maritime Technology, Toyama*

<sup>51</sup>*University of Tsukuba, Tsukuba*

<sup>52</sup>*Utkal University, Bhubaneswer*

<sup>53</sup>*Virginia Polytechnic Institute and State University, Blacksburg VA*

<sup>54</sup>*Yokkaichi University, Yokkaichi*

<sup>55</sup>*Yonsei University, Seoul*

## Abstract

We report studies of the decay  $B^\pm \rightarrow D_{CP}K^\pm$ , where  $D_{CP}$  denotes neutral  $D$  mesons that decay to  $CP$  eigenstates. The analysis is based on a  $29.1 \text{ fb}^{-1}$  data sample of collected at the  $\Upsilon(4S)$  resonance with the Belle detector at the KEKB asymmetric  $e^+e^-$  storage ring. Ratios of branching fractions of Cabibbo-suppressed to Cabibbo-favored processes involving  $D_{CP}$  are determined to be  $\mathcal{B}(B^- \rightarrow D_1K^-)/\mathcal{B}(B^- \rightarrow D_1\pi^-) = 0.125 \pm 0.036 \pm 0.010$  and  $\mathcal{B}(B^- \rightarrow D_2K^-)/\mathcal{B}(B^- \rightarrow D_2\pi^-) = 0.119 \pm 0.028 \pm 0.006$ , where indices 1 and 2 represent the  $CP = +1$  and  $CP = -1$  eigenstates of the  $D^0 - \bar{D}^0$  system, respectively. We also extract the partial rate asymmetries for  $B^\pm \rightarrow D_{CP}K^\pm$ , finding  $\mathcal{A}_1 = 0.29 \pm 0.26 \pm 0.05$  and  $\mathcal{A}_2 = -0.22 \pm 0.24 \pm 0.04$ .

PACS numbers: 12.15.Hh, 13.25.Hw

Direct  $CP$ -violation in  $B^\pm \rightarrow D_{CP}K^\pm$  decay, where  $D_{CP}$  denotes neutral  $D$  mesons that decay to  $CP$  eigenstates, provides a promising way to extract the angle  $\phi_3$  of the Cabibbo-Kobayashi-Maskawa unitarity triangle [1, 2]. A partial rate asymmetry between the  $D_{CP}K^-$  and  $D_{CP}K^+$  final states can arise from interference between  $b \rightarrow c$  and  $b \rightarrow u$  processes shown in Fig. 1. The relation of the partial rate asymmetry  $\mathcal{A}_{CP}$  and the  $\phi_3$  angle [3] is given by:

$$\begin{aligned} \mathcal{A}_{1,2} &\equiv \frac{\mathcal{B}(B^- \rightarrow D_{1,2}K^-) - \mathcal{B}(B^+ \rightarrow D_{1,2}K^+)}{\mathcal{B}(B^- \rightarrow D_{1,2}K^-) + \mathcal{B}(B^+ \rightarrow D_{1,2}K^+)} \\ &= \frac{2r \sin \delta' \sin \phi_3}{1 + r^2 + 2r \cos \delta' \cos \phi_3}, \end{aligned} \quad (1)$$

where indices 1 and 2 denote the  $CP = +1$  and  $CP = -1$  eigenstates of the neutral  $D$  mesons,  $r$  is the ratio of the amplitudes,  $r \equiv |A(B^- \rightarrow \bar{D}^0 K^-)/A(B^- \rightarrow D^0 K^-)|$ , and  $\delta'$  is the strong phase difference between the two amplitudes, with  $\delta' = \delta$  for  $D_1$  and  $\delta' = \delta + \pi$  for  $D_2$ . This asymmetry can have a non-zero value when both  $\phi_3$  and  $\delta$  are non-zero. In principle, one can constrain the angle  $\phi_3$  from the measurement of asymmetries  $\mathcal{A}_1$  and  $\mathcal{A}_2$ .

Experimentally,  $B \rightarrow DK$  processes have been studied using measurements of the ratio of the Cabibbo-suppressed process  $B^- \rightarrow D^0 K^-$  to the Cabibbo-favored process  $B^- \rightarrow D^0 \pi^-$ . Belle [4] measured  $R = \mathcal{B}(B^- \rightarrow D^0 K^-)/\mathcal{B}(B^- \rightarrow D^0 \pi^-) = 0.079 \pm 0.009 \pm 0.006$ , while CLEO [5] reported  $R = 0.055 \pm 0.014 \pm 0.005$ . Assuming factorization,  $R$  is naively expected to be  $\tan^2 \theta_C (f_K/f_\pi)^2 \approx 0.074$  in a tree-level approximation, where  $\theta_C$  is the Cabibbo angle, and  $f_K$  and  $f_\pi$  are the decay constants. Both measurements are in agreement with this theoretical expectation.

In this Letter, we report the first measurement of  $B^\pm \rightarrow D_{CP}K^\pm$  decay. We also give a comparison of the ratio of branching fractions  $R$  for the flavor specific state and the  $CP = \pm 1$  eigenstates, and a determination of the asymmetries  $\mathcal{A}_{1,2}$ . The results are based on a  $29.1 \text{ fb}^{-1}$  data sample collected on the  $\Upsilon(4S)$  resonance with the Belle detector [6] at the KEKB asymmetric  $e^+e^-$  collider [7]. This corresponds to approximately 31.3 million  $B\bar{B}$  events. The inclusion of charged conjugate states is implied throughout this Letter unless otherwise stated.

Belle is a general-purpose detector with a 1.5 T superconducting solenoid magnet that can distinguish the Cabibbo-suppressed process  $B^- \rightarrow D^0 K^-$  from the Cabibbo-favored process  $B^- \rightarrow D^0 \pi^-$  by means of particle identification and kinematic separation. A charged-particle tracking system, covering approximately 90% of the solid angle in the center-of-mass (cm) frame, is comprised of a three-layer silicon vertex detector (SVD) and a 50-layer central drift chamber (CDC). Identification of charged hadron species is accomplished by combining responses from silica aerogel Čerenkov counters (ACC), the time-of-flight detector (TOF) and the  $dE/dx$  measurement from the CDC; it provides more than  $2.5\sigma$   $K/\pi$  separation for laboratory momenta up to  $3.5 \text{ GeV}/c$ . A CsI(Tl) Electromagnetic Calorimeter (ECL) located inside the solenoid coil is used for photon ( $\gamma$ ) detection. A detailed description of the Belle detector can be found elsewhere [6].

We analyze both  $B^- \rightarrow D^0 K^-$  and  $B^- \rightarrow D^0 \pi^-$ , which are collectively referred to as  $B^- \rightarrow D^0 h^-$  decays. The processes  $B^- \rightarrow D^0 K^-$  and  $B^- \rightarrow D^0 \pi^-$  are distinguished by a tight requirement on the particle identification of the prompt  $h^-$  ( $K^-$  or  $\pi^-$ ) and the effect of the mass difference at the final stage of the event selection. The decay  $B^- \rightarrow D^0 \pi^-$  is used as a control sample to establish constraints on kinematic variables, resolution of detectors, evaluation of systematic uncertainties and normalization of results.

Flavor specific  $D^0$  meson candidates are reconstructed via  $D_f \rightarrow K^- \pi^+$ ; for  $CP = +1$  eigenstates we use  $D_1 \rightarrow K^- K^+$  and  $\pi^- \pi^+$  and for  $CP = -1$  we use  $D_2 \rightarrow K_S \pi^0$ ,  $K_S \omega$ ,  $K_S \phi$ ,  $K_S \eta$  and  $K_S \eta'$ .

The  $K_S \rightarrow \pi^+ \pi^-$  candidates are reconstructed from two oppositely charged tracks with an invariant mass within  $\pm 3\sigma$  of the nominal  $K_S$  mass. Candidate  $\pi^0$  mesons are reconstructed from pairs of  $\gamma$ 's, each with energy greater than 30 MeV, and are required to have a reconstructed mass within  $\pm 3\sigma$  of the nominal  $\pi^0$  mass. We form candidate  $\eta$  and  $\eta'$  mesons using the  $\gamma\gamma$  and  $\eta\pi^+\pi^-$  decay modes with mass ranges of  $0.495 \text{ GeV}/c^2 < M(\gamma\gamma) < 0.578 \text{ GeV}/c^2$  and  $0.904 \text{ GeV}/c^2 < M(\eta\pi^+\pi^-) < 1.003 \text{ GeV}/c^2$ , respectively. The  $\eta$  momentum is required to be greater than 500 MeV/c.

Candidate  $\omega$  and  $\phi$  mesons are reconstructed from  $\pi^+\pi^-\pi^0$  and  $K^+K^-$  combinations with invariant masses in the ranges  $0.733 \text{ GeV}/c^2 < M(\pi^+\pi^-\pi^0) < 0.819 \text{ GeV}/c^2$  and  $1.007 \text{ GeV}/c^2 < M(K^+K^-) < 1.031 \text{ GeV}/c^2$ , respectively. A helicity angle requirement for the  $\omega$  and  $\phi$  mesons of  $|\cos \theta_{hel}| > 0.4$  reduces the contributions from non-resonant  $D^0 \rightarrow K_S \pi^+ \pi^- \pi^0$  and  $K_S K^+ K^-$  decays to a negligible level. For  $D^0 \rightarrow K_S \omega$ , the  $D^0 \rightarrow K^{*-} \rho^+$  background is explicitly rejected by vetoing any  $K_S \pi^-$  combination that forms an invariant mass within  $\pm 75 \text{ MeV}/c^2$  of the nominal  $K^*$  mass.

For each charged track from the  $D^0$  meson decay, the particle identification system is used to determine a  $K/\pi$  likelihood ratio  $P(K/\pi) = \mathcal{L}_K / (\mathcal{L}_K + \mathcal{L}_\pi)$ , where  $\mathcal{L}_K$  and  $\mathcal{L}_\pi$  are kaon and pion likelihoods [6]. For  $D^0 \rightarrow K^- \pi^+$ ,  $K^- K^+$ , and  $\pi^- \pi^+$ , the charged tracks with  $P(K/\pi) < 0.7$  are assigned to be pions, while kaons are required to satisfy  $P(K/\pi) > 0.3$  for  $D^0 \rightarrow K^- \pi^+$  and  $P(K/\pi) > 0.7$  for  $D^0 \rightarrow K^- K^+$ . Pions from candidate  $D^0 \rightarrow \pi^- \pi^+$  decays are required to have momentum greater than 0.8 GeV/c, and the candidate is vetoed if either pion, when combined with any other track in the event, has an invariant mass that is within  $\pm 50 \text{ MeV}/c^2$  of the nominal  $J/\psi$  mass, or within  $\pm 20 \text{ MeV}/c^2$  of the nominal  $D^0$  mass.

Candidate  $D^0$  mesons are also required to have an invariant mass within  $\pm 2.5\sigma$  of the nominal  $D^0$  mass, where  $\sigma$  is the measured mass resolution, which ranges from 5 to 18 MeV/c<sup>2</sup>, depending on the decay channel. Tracks and photons from the  $D^0$  candidate final states, except for  $K_S \pi^0$ ,  $K_S \eta$  and  $K_S \eta'$ , are refitted according to the nominal  $D^0$  meson mass hypothesis and the reconstructed vertex position, in order to improve momentum determination.

We reconstruct  $B^- \rightarrow Dh^-$  events using the laboratory constrained mass ( $M_{lc}$ ).  $M_{lc}$  is the  $B$  candidate mass calculated from the laboratory momenta by using an  $e^+e^- \rightarrow B\bar{B}$  hypothesis:  $M_{lc} = \sqrt{(E_B^{lab})^2 - (p_B)^2}$ , where  $p_B$  is the  $B$  candidate's laboratory momentum vector and  $E_B^{lab} = \frac{1}{E_{ee}}(s/2 + \mathbf{P}_{ee} \cdot \mathbf{P}_B)$ , where  $s$  is square of the cm energy,  $\mathbf{P}_B$  is the laboratory momentum vector of the  $B$  meson candidate, and  $\mathbf{P}_{ee}$  and  $E_{ee}$  are the laboratory momentum and energy of the  $e^+e^-$  system, respectively.  $M_{lc}$  is independent of the mass assumption of the particle to be used, and is suitable for both  $B^- \rightarrow D\pi^-$  and  $B^- \rightarrow DK^-$  simultaneously. We accept  $B$  candidates with  $5.27 \text{ GeV}/c^2 < M_{lc} < 5.29 \text{ GeV}/c^2$ .

Background events from  $e^+e^- \rightarrow q\bar{q}$  continuum processes are rejected using event shape variables that distinguish between spherical  $B\bar{B}$  events and jet-like continuum events. We construct a Fisher discriminant,  $\mathcal{F} = \sum_{l=2,4} \alpha_l R_l^{so} + \sum_{l=1}^4 \beta_l R_l^{oo}$ , where  $\alpha_l$ ,  $\beta_l$  are optimized coefficients to maximize the discrimination between  $B\bar{B}$  events and continuum events, and  $R_l^{so}$ ,  $R_l^{oo}$  are modified Fox-Wolfram moments [11] [12]. Furthermore, the variable  $\cos \theta_B$  is used, where  $\theta_B$  is the angle between the  $B$  flight direction in the  $\Upsilon(4S)$  rest frame and the beam axis. A single likelihood variable is formed from the probability density functions of

$\mathcal{F}$  and  $\cos\theta_B$ . The likelihood ratio is defined as  $\mathcal{LR} = \mathcal{L}_{\text{sig}}/(\mathcal{L}_{\text{sig}} + \mathcal{L}_{\text{cont}})$  where  $\mathcal{L}_{\text{sig}}$  and  $\mathcal{L}_{\text{cont}}$  are likelihoods defined by  $\mathcal{F}$  and  $\cos\theta_B$  for the signal and continuum background, respectively. Since each  $D^0$  sub-decay mode has different backgrounds, we optimize the cut of the likelihood ratio for each mode by maximizing  $S/\sqrt{S+N}$ , where  $S$  and  $N$  denote the numbers of signal and background events estimated by a Monte Carlo simulation [10]. For the  $D^0 \rightarrow K^-\pi^+$  mode, the requirement  $\mathcal{LR} > 0.4$  retains 87.1% of signal and 26.4% of the continuum background.

To distinguish between  $B^- \rightarrow D^0K^-$  and  $B^- \rightarrow D^0\pi^-$  processes, we form two samples by requiring that the prompt hadron  $h^-$  satisfies either  $P(K/\pi) > 0.8$  ( $B^- \rightarrow D^0K^-$  enriched sample) or  $P(K/\pi) < 0.8$  ( $B^- \rightarrow D^0\pi^-$  enriched sample). Finally, the  $\Delta E$  distribution, calculated by assigning the pion mass to the prompt hadron  $h^-$ , is examined to distinguish between  $B^- \rightarrow D^0K^-$  and  $B^- \rightarrow D^0\pi^-$  processes, where  $\Delta E$  is the energy difference in the cm frame:  $\Delta E = E_D^{cm} + E_{h^-}^{cm} - E_{\text{beam}}^{cm}$ . The signals for  $B^- \rightarrow D^0\pi^-$  and  $B^- \rightarrow D^0K^-$  peak in the  $\Delta E$  distributions at 0 MeV and -49 MeV respectively, as can be seen in Fig. 2. In the  $B^- \rightarrow D^0K^-$  enriched sample, we can also see a peak around  $\Delta E = 0$  MeV due to misidentified pions from  $B^- \rightarrow D^0\pi^-$  in Fig. 2(b), (d), and (f).

The numbers of  $B^- \rightarrow D^0\pi^-$  and  $B^- \rightarrow D^0K^-$  events are extracted by fitting double Gaussian functions with different central values and widths to the  $\Delta E$  distribution. Backgrounds originate from  $q\bar{q}$  continuum events and  $B\bar{B}$  events. Continuum events are distributed over the entire  $\Delta E$  region, and the shape of this background is determined by fitting a linear function to the  $\Delta E$  distribution in the  $M_{l_c}$  sideband region ( $5.20 \text{ GeV}/c^2 < M_{l_c} < 5.26 \text{ GeV}/c^2$ ).  $B\bar{B}$  backgrounds, such as  $B^- \rightarrow D^0\rho^-$  and  $B \rightarrow D^*\pi^-$  processes, are mostly seen at negative values of  $\Delta E$ ; MC simulations are used to obtain the shape of their distribution.

In the fits to the  $B^- \rightarrow D^0\pi^-$  enriched  $\Delta E$  distribution, the signal peak position and width, and the normalization of continuum and  $B\bar{B}$  backgrounds are free parameters. On the other hand, we calibrated the shape parameters of the  $B^- \rightarrow D^0K^-$  signal using the  $B^- \rightarrow D^0\pi^-$  data following the procedure described in [4], which accounts for the kinematical shifts and smearing of the  $\Delta E$  peaks caused by the incorrect mass assignments of prompt hadrons. For the  $B^- \rightarrow D^0K^-$  fit, the shape parameters of the double Gaussian of the signal are fixed at values determined from the fit to the  $B^- \rightarrow D^0\pi^-$  sample. The peak position and width of the  $B^- \rightarrow D^0K^-$  signal events are determined by fitting the  $B^- \rightarrow D^0\pi^-$  distribution using a kaon mass hypothesis for the prompt pion, where the relative peak position is reversed with respect to the origin. The shape parameters for the feed-across from  $B^- \rightarrow D^0\pi^-$  is fixed by the fit results of the  $B^- \rightarrow D^0\pi^-$  enriched sample.

The fit results are shown as solid curves in Fig. 2. The number of events in the  $D^0K^-$  signal and  $D^0\pi^-$  feed-across, and the statistical significance of the  $D^0K^-$  signal are given in Table I. The statistical significance is defined as  $\sqrt{-2 \ln(\mathcal{L}_0/\mathcal{L}_{max})}$ , where  $\mathcal{L}_{max}$  is the maximum likelihood in the  $\Delta E$  fit and  $\mathcal{L}_0$  is the likelihood when the signal yield is constrained to be zero. The statistical significance of both  $D_1K^-$  and  $D_2K^-$  signals is over  $5.0\sigma$ .

Experimentally, the ratio of branching fractions is determined as follows:

$$R = \frac{N(B^- \rightarrow D^0K^-)}{N(B^- \rightarrow D^0\pi^-)} \times \frac{\eta(B^- \rightarrow D^0\pi^-)}{\eta(B^- \rightarrow D^0K^-)} \times \frac{\epsilon(\pi)}{\epsilon(K)}, \quad (2)$$

where  $N$  is the number of events obtained,  $\eta$  is the signal detection efficiency, and  $\epsilon$  is the prompt pion or kaon identification efficiency. The signal detection efficiencies are determined from MC simulation:  $\eta(B^- \rightarrow D^0K^-)$  is approximately 5% lower than  $\eta(B^- \rightarrow D^0\pi^-)$

due to kaon decays in flight. Kaon and pion identification efficiencies  $\epsilon(K)$  and  $\epsilon(\pi)$  are experimentally determined from a kinematically selected sample of  $D^{*+} \rightarrow D^0\pi^+$  and  $D^0 \rightarrow K^-\pi^+$  decays with  $K^-$  and  $\pi^+$  mesons from  $D^0$  candidates that are in the same cm momentum ( $p^{cm}$ ) and polar angle regions as prompt hadrons in the  $B^- \rightarrow Dh^-$  decay ( $2.1 \text{ GeV}/c < p^{cm} < 2.5 \text{ GeV}/c$ ). With our requirements,  $P(K/\pi) > 0.8$  gives a kaon identification efficiency of  $\epsilon(K) = 0.778 \pm 0.005$  with a pion misidentification rate of  $0.024 \pm 0.002$ , and  $P(K/\pi) < 0.8$  gives a pion identification efficiency of  $\epsilon(\pi) = 0.972 \pm 0.007$ .

Since the kinematics of the  $B^- \rightarrow D^0K^-$  and  $B^- \rightarrow D^0\pi^-$  processes are similar, the systematic uncertainties from detection efficiencies cancel in the ratios of branching fractions. The dominant systematic errors are the uncertainties in the shapes of backgrounds in the  $\Delta E$  distributions (5.1% – 7.9%), which are determined by varying the background shape of the fitting function by  $\pm 1\sigma$ , and  $K/\pi$  identification efficiencies (1.2%). The sum of the uncertainties for each mode are combined in quadrature to determine the total systematic errors for the ratios.

The resulting measurements of  $R$  are listed with their statistical and systematic errors in Table I. These are the first observations of the decays  $B^- \rightarrow D_{CP}K^-$ . As a check, the result for the flavor specific decay  $B^- \rightarrow D^0h^-, D^0 \rightarrow K^-\pi^+$  is listed as well, and is found to be consistent with previous measurements. We find no deviation of the  $R$  ratio for the  $B^- \rightarrow D_{CP}K^-$  processes from the corresponding flavor specific modes beyond statistical errors.

Direct  $CP$  violation is investigated by measuring the partial rate asymmetries in  $B^\pm \rightarrow D_{1,2}K^\pm$  decays. We fit the yields of  $B^+$  and  $B^-$  events separately for each mode and determine the partial rate asymmetries  $\mathcal{A}_{1,2}$  are shown in Table II. The partial rate asymmetry is consistent with zero for the flavor specific mode, which is expected to have no asymmetry. To construct 90% confidence intervals of  $\mathcal{A}_1$  and  $\mathcal{A}_2$ , we combine statistical and systematic errors in quadrature, and assume that the total error is distributed as a Gaussian. We find  $-0.14 < \mathcal{A}_1 < 0.73$  and  $-0.62 < \mathcal{A}_2 < 0.18$ , consistent with zero asymmetry.

The main sources of systematic errors for the partial rate asymmetries  $\mathcal{A}_{1,2}$  are asymmetries in the measured background (1.5% – 3.9%), intrinsic asymmetry in the Belle detector (3.6%), and kaon identification (1.0%). We observe  $1154.6 \pm 35.4 B^+ \rightarrow \bar{D}^0\pi^+, \bar{D}^0 \rightarrow K^+\pi^-$  candidates and  $1073.5 \pm 34.5 B^- \rightarrow D^0\pi^-, D^0 \rightarrow K^-\pi^+$  candidates. This is consistent with our expectation that the detector has no significant intrinsic charge asymmetry. Using MC simulation, we find that the contribution of the non-resonant contaminations ( $\sim 0.1\%$ ) of  $\omega$  and  $\phi$  can be neglected.

In conclusion, using  $29.1 \text{ fb}^{-1}$  of data collected with the Belle detector, we report studies of the decays  $B^\pm \rightarrow D_{CP}K^\pm$ , where  $D_{CP}$  are the neutral  $D$  meson  $CP$  eigenstates. This is the first stage of a program to measure the angle  $\phi_3$  in the CKM unitarity triangle. The ratios of branching fractions  $R$  for the decays  $B^- \rightarrow D_{CP}K^-$  and  $B^- \rightarrow D_{CP}\pi^-$  are consistent with that for the flavor specific decay within errors. The measured partial rate asymmetries  $\mathcal{A}_{1,2}$  are consistent with zero within large errors. In the future, with  $300 \text{ fb}^{-1}$  of data, an accuracy of better than 0.1 in the measurements of  $R_{1,2}$  and  $\mathcal{A}_{1,2}$  in  $B^- \rightarrow D_{CP}K^-$  is expected and we will begin to constrain the angle  $\phi_3$ .

We wish to thank the KEKB accelerator group for the excellent operation of the KEKB accelerator. We acknowledge support from the Ministry of Education, Culture, Sports, Science, and Technology of Japan and the Japan Society for the Promotion of Science; the Australian Research Council and the Australian Department of Industry, Science and Resources; the Department of Science and Technology of India; the BK21 program of the Ministry of

Education of Korea and the CHEP SRC program of the Korea Science and Engineering Foundation; the Polish State Committee for Scientific Research under contract No.2P03B 17017; the Ministry of Science and Technology of Russian Federation; the National Science Council and the Ministry of Education of Taiwan; the Japan-Taiwan Cooperative Program of the Interchange Association; National Science Foundation of China under Contract No. 10175071; and the U.S. Department of Energy.

\* on leave from Nova Gorica Polytechnic, Nova Gorica

- [1] M. Gronau and D. Wyler, Phys. Lett. **B265** 172 (1991).  
 [2] I. Dunietz, Phys. Lett. **B270** 75 (1991); D. Atwood, I. Dunietz and A. Soni, Phys. Rev. Lett. **78** 3257 (1997).  
 [3] H. Quinn and A.I. Sanda, Eur. Phys. J. **C15** 626 (2000).  
 [4] K. Abe *et al.* (Belle Collaboration), Phys. Rev. Lett. **87** 111801 (2001).  
 [5] M. Athanas *et al.* (CLEO Collaboration), Phys. Rev. Lett. **80** 5493 (1998).  
 [6] A. Abashian *et al.* (Belle Collaboration), Nucl. Instr. and Meth. **A479**, 117 (2002).  
 [7] KEKB B-factory Design Report, KEK Report 95-7 (1995), unpublished.  
 [8] The charge conjugated mode ( $\bar{D}^0 \rightarrow K^+\pi^-$ ) is implicitly included.  
 [9] The  $\omega$  helicity angle is defined as the angle between the  $D^0$  flight direction in the  $\Upsilon(4S)$ 's frame and the normal to the  $\omega$  decay plane in the  $\omega$ 's rest frame. The  $\phi$  helicity angle is defined as the angle between the  $\phi$  flight direction in the  $D$ 's rest frame and the direction of the  $\phi$ 's daughter in the  $\phi$ 's rest frame.  
 [10] We use the QQ  $B$ -meson decay event generator developed by the CLEO Collaboration (<http://www.lns.cornell.edu/public/CLEO/soft/QQ>) and GEANT3 for the detector simulation; CERN Program Library Long Writeup W5013, CERN, 1993  
 [11] K. Abe *et al.* (Belle Collaboration), Phys. Rev. Lett. **87**, 101801 (2001).  
 [12] The index *so(oo)* indicates that the moment is calculated from pairs of particles where only one (neither) particle comes from the  $B$  candidate.

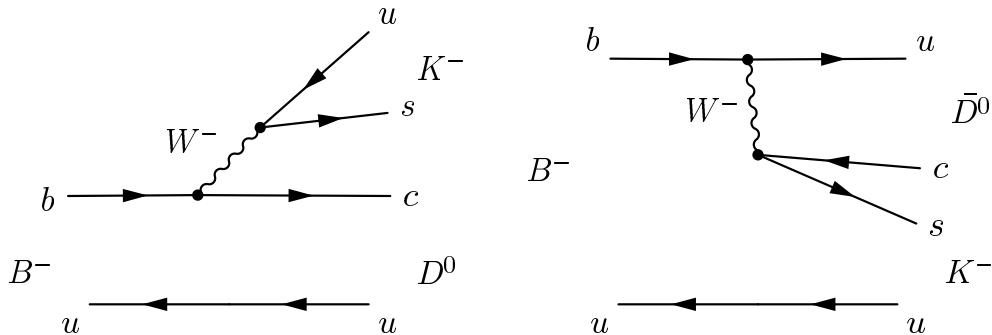


FIG. 1:  $B^- \rightarrow D^0 K^-$  decay amplitudes.



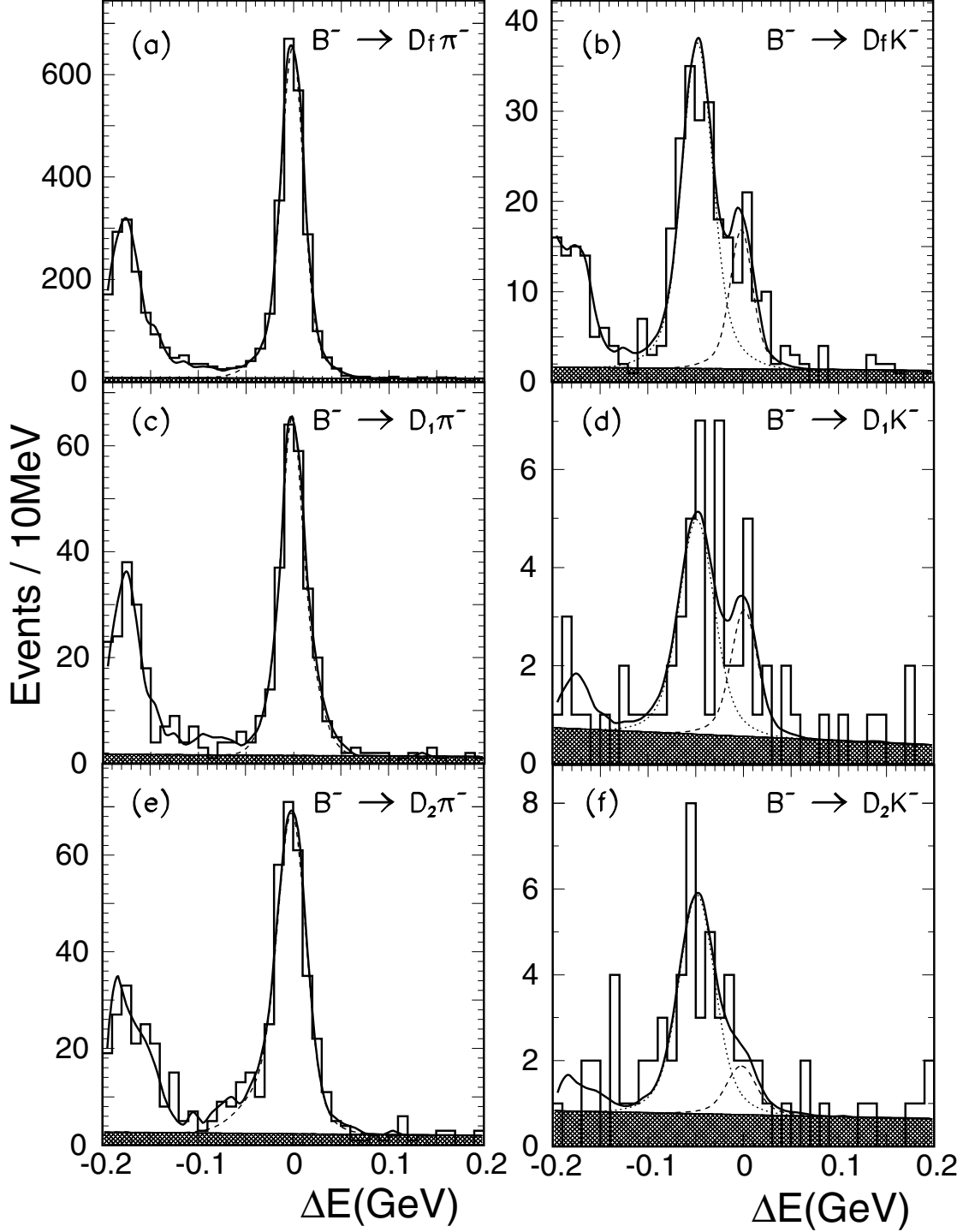


FIG. 2:  $\Delta E$  distributions for  $B^- \rightarrow D^0 \pi^- / K^-$  candidates and fit results: (a)  $B^- \rightarrow D_f \pi^-$ , (b)  $B^- \rightarrow D_f K^-$ , (c)  $B^- \rightarrow D_1 \pi^-$ , (d)  $B^- \rightarrow D_1 K^-$ , (e)  $B^- \rightarrow D_2 \pi^-$ , and (f)  $B^- \rightarrow D_2 K^-$ , where in each case the pion mass is assigned to the prompt  $\pi^- / K^-$ . Dotted (dashed) lines show the distributions of  $DK(D\pi)$  signals. The shaded plot shows the continuum background and the remaining component from  $B\bar{B}$  background is estimated and fitted by Monte Carlo simulation. In the  $DK$  plots, the dashed curves show the  $D^0 \pi$  feed-across.

TABLE I: Results of fits for the  $D^0\pi^-$  and  $D^0K^-$  decay modes. The event yields, the feed-across from  $D^0\pi^-$  to the  $D^0K^-$  signal region, statistical significance of  $D^0K^-$  signals, efficiencies and branching fraction ratios( $R$ ) are given. Efficiencies are determined by weighting according to the measured sub-components ( $\eta \equiv \sum_i \eta_i \mathcal{B}(D^0 \rightarrow X_i)$ ).

	$B^- \rightarrow D^0K^-$ events	$B^- \rightarrow D^0\pi^-$ feed-across	Stat. sig.	$B^- \rightarrow D^0\pi^-$ events	Efficiency(%) $\eta(D^0\pi^-)/\eta(D^0K^-)$	branching fraction ratio $R$
$B^- \rightarrow D_f h^-$	$161.7 \pm 14.5$	$51.3 \pm 9.7$	16.9	$2245.1 \pm 51.0$	1.703/1.639	$0.094 \pm 0.009 \pm 0.007$
$B^- \rightarrow D_1 h^-$	$22.9 \pm 6.1$	$9.6 \pm 4.4$	5.1	$240.1 \pm 16.7$	0.173/0.165	$0.125 \pm 0.036 \pm 0.010$
$B^- \rightarrow D_2 h^-$	$26.1 \pm 6.5$	$4.9 \pm 4.1$	5.5	$290.6 \pm 19.1$	0.184/0.173	$0.119 \pm 0.028 \pm 0.006$

TABLE II: Summary of measured partial rate asymmetries.

Mode	$N(B^+)$	$N(B^-)$	$\mathcal{A}_{CP}$	90% C.L.
$B^\pm \rightarrow D_f K^\pm$	$80.6 \pm 10.1$	$81.1 \pm 10.4$	$0.003 \pm 0.089 \pm 0.037$	$-0.15 < \mathcal{A}_f < 0.16$
$B^\pm \rightarrow D_1 K^\pm$	$8.1 \pm 3.9$	$14.7 \pm 4.6$	$0.29 \pm 0.26 \pm 0.05$	$-0.14 < \mathcal{A}_1 < 0.73$
$B^\pm \rightarrow D_2 K^\pm$	$16.4 \pm 5.5$	$10.6 \pm 4.2$	$-0.22 \pm 0.24 \pm 0.04$	$-0.62 < \mathcal{A}_2 < 0.18$